Int J Thermophys (2008) 29:93–103
DOI 10.1007/s10765-007-0344-2

Assembly and Study of Different Mercury Cells with Known Impurity Content and Isotopic Composition

D. del Campo · V. Chimenti · J. Reyes · J. A. Rodríguez Castrillón · M. Moldovan · J. I. García Alonso

Published online: 8 January 2008

Abstract The "Centro Español de Metrología" is carrying out a project to improve the knowledge of the influence of impurities and isotopic composition on the temperature of the mercury triple point. High-purity mercury from the Almaden mine (stated purity of 99.9998%) was further purified by vacuum distillation. Three mercury fractions, the original mercury from Almaden and two distilled fractions, were characterized in terms of both impurities and isotopic composition and used to measure the mercury triple point. The original mercury sample contained silver at $560\,\mathrm{ng}\cdot\mathrm{g}^{-1}$ as the main impurity while the impurity levels were much lower (silver $< 1\,\mathrm{ng}\cdot\mathrm{g}^{-1}$) in the two distilled fractions. The isotopic composition of the distilled fractions showed delta values, expressed as $1{,}000\times(^{198/202}\mathrm{Hg}_{\mathrm{sample}} - ^{198/202}\mathrm{Hg}_{\mathrm{reference}})/^{198/202}\mathrm{Hg}_{\mathrm{reference}}$, of 1.37 ± 0.07 (1σ) for the first distilled sample and -1.55 ± 0.03 (1σ) for the second distilled sample with reference to the original Almaden mercury. For the measurement of the mercury triple point, an alcohol stirred bath was used that allowed two cells to be compared nearly simultaneously. It was observed that the presence of the silver impurities in the high-purity mercury modified slightly the mercury triple point while the effect of variations in the isotopic composition can be considered negligible.

Keywords Impurities · Isotopic composition · Triple point of mercury

D. del Campo (✉) · V. Chimenti
Centro Español de Metrología, Alfar, 2, 28760 Tres Cantos, Spain
e-mail: ddelcampo@cem.mityc.es

J. Reyes
Instituto Geológico y Minero de España, La Calera, 1, 28760 Tres Cantos, Spain

J. A. R. Castrillón · M. Moldovan · J. I. García Alonso
Departamento de Química Física y Analítica, Universidad de Oviedo, Julián Clavería, 8, 33006 Oviedo, Spain

1 Introduction

Within the framework of the EUROMET Project 732 "Toward More Accurate Fixed Points," the "Centro Español de Metrología" has focused on evaluating the effects of impurities and isotopic composition on the triple point of mercury [1]. It is well known that minor impurities may affect the measured triple point and that the isotopic composition of the material may be changed by the purification procedure. To some extent, these issues are still controversial and the solution is not trivial [1–3]. In order to understand and quantify these additional sources of uncertainty, thermal measurements alone are insufficient; it is essential to carry out chemical metrology measurements to quantify the impurity concentrations and isotopic composition [4,5]. In this work, we have characterized the concentrations of metallic impurities and the isotopic compositions of two mercury samples obtained by vacuum distillation of a high-purity mercury sample obtained from the Almaden mine. Triple-point measurements were carried out on all samples.

2 The Cells: Assembly, Characterization, and Comparison

The apparatus to purify the mercury and clean and fill the cells was adapted from [6–9]. Borosilicate glass was chosen as the material for both the distillation apparatus (Fig. 1) and the cells (Fig. 2). The first cell (identified as A1P1) was filled with the mercury obtained directly from the supplier using the "fill and pump" method. The cell was gently vibrated and rotated during the evacuation process to remove the air bubbles formed inside the cell. Two additional cells were filled under controlled vacuum distillation. To prevent any emission of mercury vapor, a cold trap and a carbon

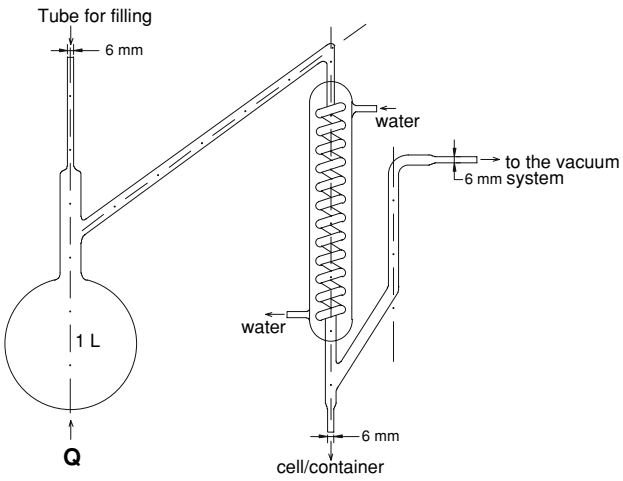

Fig. 1 Distillation apparatus design

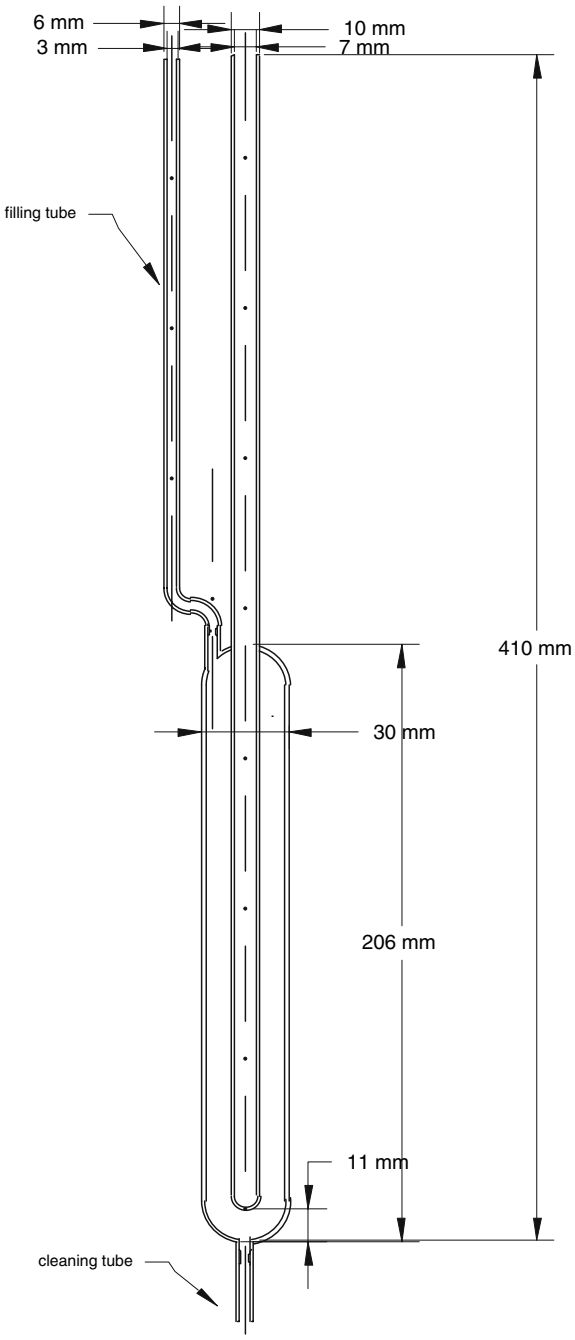

Fig. 2 Cell design

filter in the vacuum pump were used during the distillation process. Finally, three cells containing about 1.5 kg of mercury and providing more than 19 cm of total immersion depth in the thermometric well were assembled.

2.1 Distillation Process

The distillation process was carried out to force isotopic fractionation. For this purpose, 5804.68 g of high-purity Almaden mercury was distilled at 240 °C under vacuum conditions. During the distillation process, several glass ampoules (ca. 150 g Hg), cells (ca. 1,500 g Hg), and reservoirs (for further distillation) were filled, following the order described in Table 1. At the beginning of the first distillation, cell A1P2D2 was filled, so it should be enriched in the lighter isotopes relative to the original mercury that was used to fill the first cell, A1P1. The purpose of filling the ampoules and reservoirs, previously cleaned in the same way as the cells, was to obtain mercury samples for future chemical analysis and re-distillations.

In the second stage, the distillation apparatus was cleaned again, and the mercury contained in the reservoir identified as A1P2D4 in Table 1 (containing 2569.23 g of Hg) was poured into the flask and re-distilled. As the mercury contained in this reservoir was obtained at the end of the first distillation, it should be enriched in the heavier isotopes. From this second distillation, several samples were taken as indicated in Table 2. The cell A1P4D1 was filled at the end of this stage so that it would be enriched in the heavier isotopes contained in the reservoir. The elapsed time to fill cell A1P2D2 was 5 h, and it took 6.5 h to fill cell A1P4D1. The characteristics of the three cells that were filled are summarized in Table 3.

Table 1 Summary of the first distillation process

Type of container	ID	Mercury mass (g)
Ampoule	A1P2D1a	160.81
Ampoule	A1P2D1b	143.24
Cell	A1P2D2	1507.18
Ampoule	A1P2D3a	149.90
Ampoule	A1P2D3b	154.52
Reservoir	A1P2D4	2569.23
Ampoule	A1P2D5a	134.39
Ampoule	A1P2D5b	160.31
Reservoir	A1P2D6	844.82

Table 2 Summary of the second distillation process

Type of container	ID	Mercury mass (g)
Cell	A1P4D1	1656.89
Ampoule	A1P4D2	285.98
Ampoule	A1P4D3	128.97
Reservoir	A1P4D4	458.30

Table 3 Characteristics of the assembled cells

Cell ID	Immersion depth (cm)	Mercury mass (g)
A1P1 Not distilled Hg	19.4	1515.23
A1P2D2 1st distillation	19.7	1507.18
A1P4D1 2nd distillation	19.8	1656.89

2.2 Characterization of the Cells

The shapes of the freezing and melting plateaux realized for a fixed-point cell are not recommended as a means to assess its impurity content [2,10], but such freezing and melting ranges may give an approximate idea of what might be expected. Comparing the slow melting plateau realized following a fast freeze with one following a slow freeze (provided no liquid–solid interface formed around the thermometric well) enables a qualitative analysis of this source of uncertainty. Figure 3 shows this comparison for the three mercury cells assembled; the plateaux were obtained in a stirred alcohol bath controlled at a temperature of 0.2 °C above the triple point. In order to facilitate a comparison of the melting curves, the plateaux are represented as a function of the melted fraction of mercury, F. This qualitative analysis would not be useful if a specific impurity has greater solubility in the solid state than in the liquid state of mercury, but this behavior is not expected for the major metallic impurities of mercury [11,12].

A fast freeze creates a uniform distribution of impurities; on the contrary, a slow freeze (from the outside of the cell toward the center) causes impurities more soluble in the liquid than in the solid to increase in concentration toward the thermometric well as they are rejected by the solid and forced ahead by the advance of the liquid–solid interface. As a consequence, the temperature sensed by the thermometer during a subsequent induced melting will be clearly influenced by the thermal history and by the impurity concentration of the fixed-point cell. In short, the greater the impurity concentration, the larger the differences in the shapes of the melting curves following fast and slow freezes.

Therefore, the graphs in Fig. 3 suggest a significant impurity content of cell A1P1 when compared with the other two. The measurements were performed using a 25 Ω Tinsley standard platinum-resistance thermometer and an ASL F900 bridge.

2.3 Results of the Comparison

To reduce the uncertainty due to the spurious thermal fluxes that are the dominant influences on the melting and freezing curves if the impurities are not taken into account, the cells were compared in pairs in the same bath, essentially, simultaneously. A copper container was used (see Fig. 4) to hold the cells, allowing the positioning of the two cells in the bath to be reproducible and facilitated the study of the alcohol thermal profile close to the cells. More than 12 different measurements of 3 different plateaux were recorded and corrected for self-heating and immersion depth. The result appears in Fig. 5 where the cell A1P2D2 has been chosen as the reference. The error bars of Fig. 5 were estimated by taking into account all the sources of uncertainty relevant to the comparison of artifacts; neither the impurity nor the isotopic composition influences were included in the uncertainty.

3 Impurity Analysis

The mercury remaining in the flasks was analyzed after the distillation process. This was intended to characterize the cells previously assembled. Therefore, to characterize

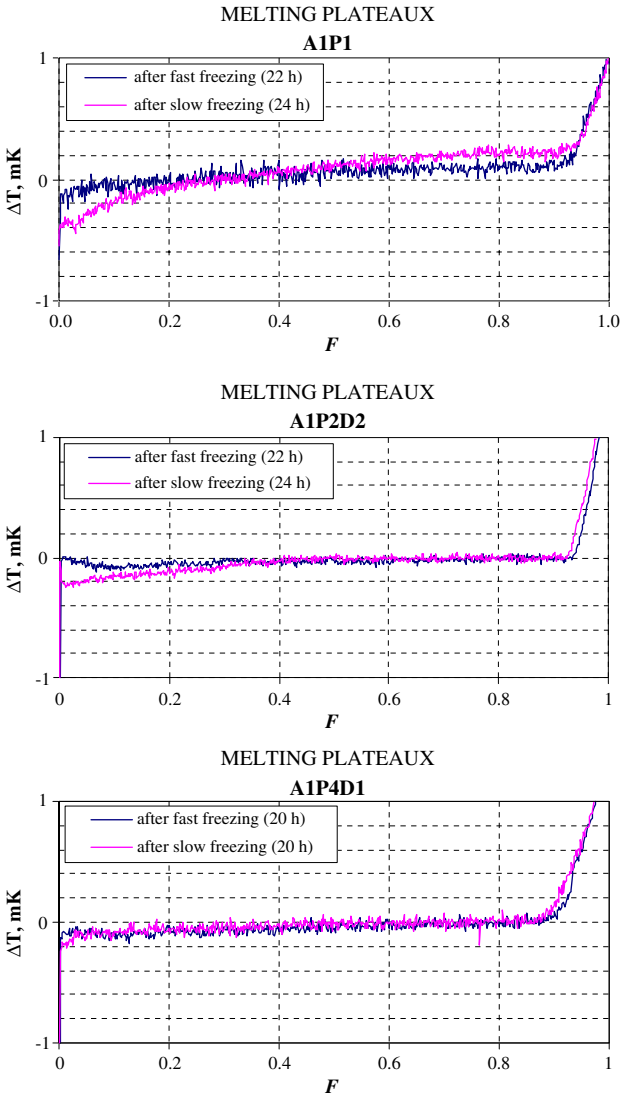

Fig. 3 Melting plateaux of the three mercury cells assembled after fast and slow freezing

the cell identified as A1P4D1, the mercury contained in the ampoule A1P4D2 was distilled a third time and its residue analyzed. The residue of the distilled mercury was dissolved with sub-distilled concentrated HNO_3 in successive washings, the final volume depending on the initial amount of mercury. The final concentration was 2% HNO_3. A blank solution was prepared by performing the preparation without any sample present. A Varian Vista MPX-AX inductively coupled plasma atomic emission spectrometer was used for the measurements. The operating parameters are listed in Table 4. The measurements were carried out with multi-elemental calibration

Fig. 4 Copper container used in the cell comparison

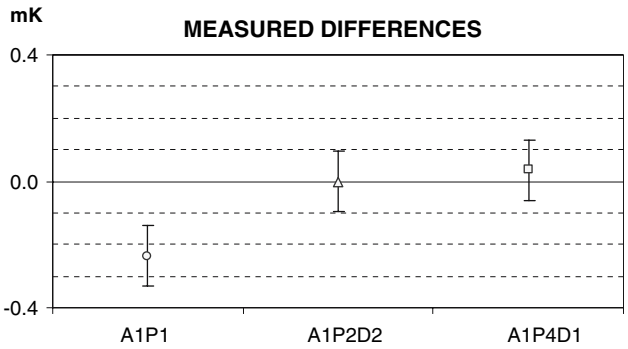

Fig. 5 Result of the comparison between the assembled cells

standard solutions and the maximum relative standard deviation (assessed on the basis of repeatability, omitting any potential unknown systematic effects) was 5%. The analytical wavelengths used and detection limits are listed in Table 5.

3.1 Results

The impurity concentrations in cells A1P1 and A1P2D2 are summarized in Tables 6 and 7 where, at the bottom, there appears the overall maximum estimate [2] for the

Table 4 ICP-AES operating conditions

Nebulizer type	V-groove
Nebulizer pressure	220 kPa
Plasma power	1.2 kW
Torch	Quartz
Plasma flow rate	15.0 $L \cdot min^{-1}$
Auxiliary flow rate	1.5 $L \cdot min^{-1}$
Pump rate	20 rpm
Integration time	10 s
Replicate	5 s
Viewing height	Optimized on SBR
Background correction	Dynamic

Table 5 ICP-AES wavelengths used and instrumental detection limits

Element	Wavelength (nm)	Detection limit ($\mu g \cdot L^{-1}$)
Ag	328.068	20
Al	396.152	50
As	188.980	20
B	249.772	50
Ba	230.424	5
Be	313.142	2
Cd	214.439	2
Co	228.615	10
Cr	267.716	10
Cu	327.395	20
Fe	238.204	10
Mn	257.610	10
Ni	231.604	20
Pb	220.353	10
Sb	206.834	20
V	311.837	10
Zn	213.857	10

liquidus point depression. The results for cell A1P4D1 are all below the detection limits and are consistent with the ones obtained for cell A1P2D2.

This analysis confirms what was suspected after the study of the melting plateaux (see Fig. 3) and the result of the comparison (see Fig. 5): the cell filled using the mercury directly from the supplier's bottle (A1P1) has a significant impurity concentration relative to the cells filled with the distilled mercury. The remarkable amount of silver (see Table 6) in the A1P1 cell can be blamed for the lower temperature it realizes compared with the other two cells. This result agrees with the studies of the Ag–Hg system [13] where a eutectic reaction very near the melting point of mercury was indicated, which has the effect of decreasing the melting-point temperature.

4 Isotopic Composition of Mercury

Mercury samples from the cells A1P1, A1P2D2, and A1P4D1 (ca. 60 mg–80 mg) were dissolved in 2 g of sub-boiling nitric acid and diluted to ca. 10 g with ultra-pure

Table 6 Results of the chemical analysis of the impurities in cell A1P1

Element i	Result ($\mathrm{ng \cdot g^{-1}}$)	Mole fraction x_i
Ag	565	1.05×10^{-06}
Al	8	5.95×10^{-08}
As	3	8.03×10^{-09}
Ba	0.3	4.38×10^{-10}
Be	0.3	6.68×10^{-09}
Cd	1.9	3.39×10^{-09}
Co	2	6.81×10^{-09}
Cr	2	7.72×10^{-09}
Cu	3	9.47×10^{-09}
Fe	29	1.04×10^{-07}
Mn	2	7.30×10^{-09}
Ni	3	1.03×10^{-08}
Pb	2	1.94×10^{-09}
Sb	3	4.94×10^{-09}
V	2	7.88×10^{-09}
Zn	4	1.23×10^{-08}
	$x = 1.30 \times 10^{-06}$	
	$A_{\mathrm{Hg}} = 5.02 \times 10^{-03}\,\mathrm{K^{-1}}$	
	$\Delta T_{\mathrm{OME}} = x/A = 2.59 \times 10^{-04}\,\mathrm{K}$	

Table 7 Results of the chemical analysis of the impurities in cell A1P2D2

Element i	Result ($\mathrm{ng \cdot g^{-1}}$)	Mole fraction x_i
Ag	1	1.86×10^{-09}
Al	2	1.49×10^{-08}
As	1	2.68×10^{-09}
B	2	3.71×10^{-08}
Ba	0.2	2.92×10^{-10}
Be	0.1	2.23×10^{-09}
Cd	0.04	7.14×10^{-11}
Co	0.4	1.36×10^{-09}
Cr	0.4	1.54×10^{-09}
Cu	1	3.16×10^{-09}
Fe	0.4	1.44×10^{-09}
Mn	0.4	1.46×10^{-09}
Ni	1	3.42×10^{-09}
Pb	0.4	3.87×10^{-10}
Sb	1	1.65×10^{-09}
V	0.4	1.58×10^{-09}
Zn	0.4	1.23×10^{-09}
	$x = 7.63 \times 10^{-08}$	
	$A_{\mathrm{Hg}} = 5.02 \times 10^{-03}\,\mathrm{K^{-1}}$	
	$\Delta T_{\mathrm{OME}} = x/A = 1.52 \times 10^{-05}\,\mathrm{K}$	

water. Further dilution of the mercury stock solution was carried out with 1% (v/v) nitric acid. The isotopic composition of mercury was measured using solutions containing $1\,\mu\mathrm{g \cdot g^{-1}}$ of mercury using a Neptune multi-collector ICP-MS instrument (ThermoFisher, Bremen, Germany). Cup configuration and measuring conditions are

Table 8 Instrument operating conditions for the Neptune multi-collector ICP-MS instrument cup configuration

L4	L3	L2	L1	C	H1	H2	H3	H4
^{194}Pt	^{196}Hg–Pt	^{198}Hg	^{199}Hg	^{200}Hg	^{201}Hg	^{202}Hg	^{204}Hg–Pb	^{206}Pb

Operating conditions: RF power, 1,200 watts; Sample gas flow, 1.1 L·min^{-1}; Auxiliary gas flow, 0.6 L·min^{-1}; Cool gas flow, 16 L·min^{-1}; Nebulizer PFA, 100 µL·min^{-1}; Integration time, 4.2 s; Idle time, 1 s; Cycles and blocks, 10 cycles and 5 blocks

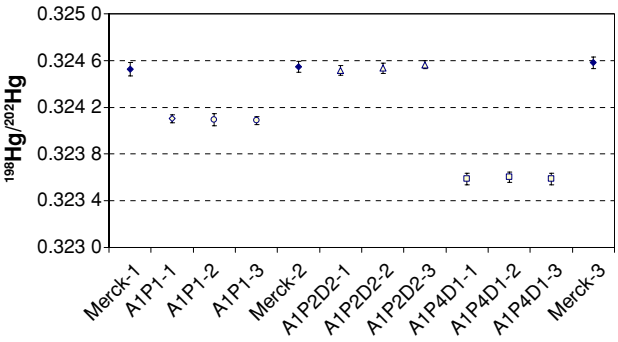

Fig. 6 Raw isotope ratios 198/202 measured for the different mercury samples

summarized in Table 8. Additionally, ^{194}Pt and ^{206}Pb were included in the cup configuration to check for metallic impurities that could affect the measurements of ^{196}Hg and ^{204}Hg due to isobaric interferences. The contributions of platinum and lead were negligible for all samples. A "natural abundance" mercury standard from Merck was used to check for mass bias drift during the measurements using the standard bracketing approach. The results obtained for the isotope ratio 198/202 of mercury are shown in Fig. 6 for triplicate measurements of the three samples and the Merck standard. As can be observed, the Merck Hg values do not change significantly during the course of the measurements and are very close to the A1P2D2 sample. The distillation process of the original sample A1P1 shows that the sample A1P2D2 is slightly enriched in the lighter isotopes while the sample A1P4D1 is enriched in the heavier isotopes. This result proves that the original purpose of the distillation process, to force isotopic fractionation, was achieved. Similar results were obtained for the other mercury isotopes. Delta values, expressed as $1{,}000\times(^{198/202}\mathrm{Hg}_{\mathrm{sample}} - ^{198/202}\mathrm{Hg}_{\mathrm{reference}})/^{198/202}\mathrm{Hg}_{\mathrm{reference}}$, using the Almaden mercury as a reference, were 1.37 ± 0.07 (1σ) for the first distilled sample and -1.55 ± 0.03 (1σ) for the second distilled sample. The difference in delta values between samples A1P2D2 and A1P4D1 and the very similar values of temperature shown in Fig. 5 indicate that variations in isotopic composition have negligible influence on the triple-point temperature of mercury.

5 Conclusion

The assembly and study of three triple-point-of-mercury cells with known and different impurity content and isotopic composition have been presented for the first time.

The chemical analyses demonstrate the presence of Ag as the dominant impurity in cell A1P1 (Table 6). This result is consistent with the thermal qualitative study performed, where cell A1P1 showed significant differences in the shapes of slow melting plateaux realized following a fast and a slow freeze (Fig. 3). It is also consistent with the predicted eutectic reaction of the Ag–Hg system [13], with the effect of decreasing the melting-point temperature as the results of the comparison performed among the three cells (Fig. 5) confirm.

The objective of the distillation process to assemble cells with different isotopic fractionation was achieved, as the analysis demonstrates (Fig. 6). It is not possible to confirm that the temperature differences observed in the comparison between the cells A1P2D2 and A1P4D1 (Fig. 5) were caused by their differences in isotopic composition due to the uncertainties associated with the constant heat flux method used in the comparison.

Next steps in the project will include a comparison among cells with different isotopic composition using an adiabatic cryostat and a detailed study of the influence of impurities on the temperature of the triple point of mercury by doping cells with controlled amounts of impurities.

References

1. G. Bonnier, E. Renaot, Y. Hermier, in *Proceedings of TEMPMEKO 2004, 9th International Symposium on Temperature and Thermal Measurements in Industry and Science*, ed. by D. Zvizdić, L.G. Bermanec, T. Veliki, T. Stašić (FSB/LPM, Zagreb, Croatia, 2004), pp. 369–376
2. D. Ripple, B. Fellmuth, M. de Groot, Y. Hermier, K.D. Hill, P.P.M. Steur, A. Pokhodum, M. Matveyev, P. Bloembergen, Working Documents of the 23rd Meeting of the Consultative Committee for Thermometry, BIPM, Document CCT/05-08 (2005)
3. D.R. White, M. Ballico, D. del Campo, S. Duris, E. Filipe, A. Ivanova, A. Kartal Dogan, E. Mendez-Lango, C.W. Meyer, F. Pavese, A. Peruzzi, E. Renaot, S. Rudtsch, K. Yamazawa, in *Proceedings of TEMPMEKO 2007*, Int. J. Thermophys. **28**, 1868 (2007) DOI: 10.1007/s10765-007-0271-2
4. K.D. Hill, S. Rudtsch, Metrologia **42**, L1 (2005)
5. F. Pavese, Metrologia **42**, 194 (2005)
6. G.T. Furukawa, in *Temperature, Its Measurement and Control in Science and Industry*, vol. 6, ed. by J.F. Schooley (AIP, New York, 1992), pp. 281–285
7. G.F. Strouse, J. Lippiatt, in *Proceedings of TEMPMEKO 2001, 8th International Symposium on Temperature and Thermal Measurements in Industry and Science*, ed. by B. Fellmuth, J. Seidel, G. Scholz (VDE Verlag, Berlin, 2002), pp. 453–458
8. K.D. Hill, Metrologia **31**, 39 (2002)
9. A.G. Steele, K.D. Hill, in *Proceedings of TEMPMEKO 2001, 8th International Symposium on Temperature and Thermal Measurements in Industry and Science*, ed. by B. Fellmuth, J. Seidel, G. Scholz (VDE Verlag, Berlin, 2002), pp. 447–452
10. B. Fellmuth, K.D. Hill, Metrologia **43**, 71 (2006)
11. Z. Galus, Pure Appl. Chem. **56**, 635 (1984)
12. C. Guminski, Polish J. Chem. **78**, 1733 (2004)
13. M.R. Baren, J. Phase Equilib. **17**, 122 (1996)